

Article

Numerical Simulation on the Safety and Quality of Cementing by Using Pad Fluid in Horizontal Wells

Ben Qi ¹, Jiawen Fu ¹, Jinfei Sun ², Zaoyuan Li ², Xin Yang ^{2,*}, Fujie Yang ² and Xuning Wu ²¹ The Second Cementing Branch of CNPC Bohai Drilling Engineering Company Limited, Tianjin 300280, China² National Key Laboratory of Oil and Gas Reservoir Geology and Exploitation, Southwest Petroleum University, Chengdu 610500, China

* Correspondence: 18628889501@163.com

Abstract: The failure of wellbore sealing will cause leakage of greenhouse gases, such as carbon dioxide and methane, which will harm oil and gas recovery and environmental safety. Cementing is an important part of wellbore sealing. Only good cementing can keep the wellbore seal for a long time and improve the well life. In this study, we considered the construction of a horizontal shale oil well in eastern China as the background and analysed the rheological properties of the annulus fluid. We developed a displacement motion model and a calculation model for the annulus dynamic equivalent circulation density, and numerical simulations were used to study the impact of the dosage and injection sequence of the pad fluid on the displacement efficiency and annulus dynamic equivalent circulation density. The results show that when the pad fluid is composed completely of flushing fluid, the displacement performance is better than that of the spacer. By increasing the dosage of the flushing fluid from 0.3 times the annular volume to 1.0 times, the displacement efficiency can be increased by 3.3%, and the retention of the drilling fluid is also reduced by 3.6%. However, it can lead to a significant reduction in the annulus dynamic equivalent circulation density and increase in the risk of leakage. After adding the spacer, the structure of the flushing fluid–spacer provides the optimal injection sequence. Considering the application status in the field example well, it was shown that it can not only ensure the safety of cementing operations, but also improve the displacement efficiency. The results of this study have important theoretical significance and application value and can provide guidance for the optimisation design of the engineering scheme.

Keywords: cementing; horizontal well; pad fluid; displacement efficiency; dynamic equivalent circulation density



Citation: Qi, B.; Fu, J.; Sun, J.; Li, Z.; Yang, X.; Yang, F.; Wu, X. Numerical Simulation on the Safety and Quality of Cementing by Using Pad Fluid in Horizontal Wells. *Energies* **2023**, *16*, 3650. <https://doi.org/10.3390/en16093650>

Academic Editors: Michael Zhengmeng Hou, Yachen Xie and Faisal Mehmood

Received: 10 March 2023

Revised: 10 April 2023

Accepted: 21 April 2023

Published: 24 April 2023



Copyright: © 2023 by the authors. Licensee MDPI, Basel, Switzerland. This article is an open access article distributed under the terms and conditions of the Creative Commons Attribution (CC BY) license (<https://creativecommons.org/licenses/by/4.0/>).

1. Introduction

In order to deal with the problem of climate change, striving to achieve carbon neutrality is the future trend [1,2]. In the field of drilling, the failure of wellbore sealing will lead to the leakage of carbon dioxide, methane and other greenhouse gases. For example, the oil spill in the Gulf of Mexico of the United [3] in 2010 and the Aliso Canyon gas leak [4] in 2015 were both caused by the failure of wellbore sealing. As a significant part of wellbore sealing, cementing plays an essential role in ensuring zonal isolation, improving wellbore stability, and preventing contamination [5]. Cementing scholars have studied on improving the sealing capacity of the cement ring in different aspects, Tan et al presented a high temperature and high density anti-corrosion cement slurry system, to ensure the sealing ability of the cement ring at high temperatures and in the presence of acidic gases of carbon dioxide and hydrogen sulphide [6]. A new solid-free resin sealant and a highly absorbent polymer have been developed for the problem of microcracks in the cement ring, to prevent the fugitive flow of fluids from forming [7,8]. The law of long-term strength attenuation of oil well cement under different curing pressures is studied [9]. According to statistics from 2019 to 2020 regarding the cementing quality of 39 shale oil wells in a region in eastern

China, it was found that the overall cementing quality is on the low side, with the rate of high-quality cementing being only 49.61%. This increases the risk of harmful gas leaks and can seriously affect wellbore life.

At present, with the deepening development of shale oil wells, the safety and quality of cementing operations are the primary prerequisites for building wellbore barriers. Figure 1 is a schematic diagram of cementing operations in a horizontal well. It is evident that when the borehole is drilled through, the casing is lowered into the well. The cement slurry (including lead and tail slurry) is displaced from the inside of the pipe to the annulus between the casing and geographic formation using the displacement fluid, which displaces the original drilling fluid. After the cement slurry solidifies, a cement sheath is formed to support the well wall and prevent the formation fluid from invading the well. The barrier that consists of cement slurry and casing near the well wall, is very critical. In consideration of the safety issues that occur during operation, if the fluid column pressure (expressed by the dynamic equivalent circulation density) generated by the flow of annulus fluid is excessive, the geographic formation can leak [10–13]. If the pressure is too low, the formation fluid can exude into the well. Meanwhile, considering the quality issues, if the displacement efficiency of the cement slurry is low, micro gaps are formed after solidification, which can also cause the failure of the wellbore sealing. All of these are the signs of failed cementing operations. To summarise, injecting pad fluid [14] (including spacer and flushing fluid) between the drilling fluid and cement slurry, can not only regulate the annulus dynamic equivalent circulation density but also increase the displacement efficiency [15–19]. Generally, the pad fluid is an intermediate fluid designed to avoid contamination from the contact between the drilling fluid and cement slurry. Therefore, the design of the pad fluid is particularly important to ensure the safety and quality of cementing operations.

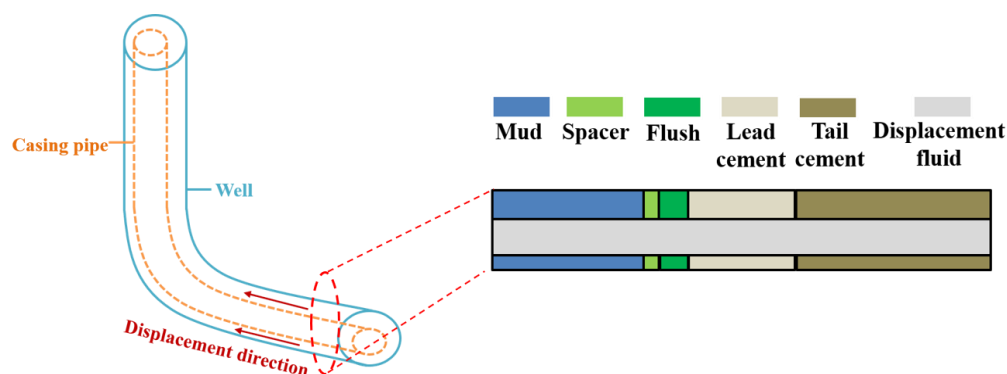


Figure 1. Schematic diagram of cementing operations in a horizontal well.

Many scholars have investigated pad fluid, and mainly focused on the pad fluid system and injection technology. In terms of the system, Chen et al. [20] developed a new cementation flushing fluid (WD-C) based on the strong flushing principle of water-soluble fibre and the oxygenolysis principle of filter cake. The results showed that the flushing fluid had an excellent washing effect on a water-based filter cake, and formed a dense network structure to improve the cementation quality of the second cementing interface. Lichinga, Kevin Nsolloh et al. [21] developed a new preflush (KV-IIA and KV -IIB) for the second cementing interface, and transformed the water-based filter cake at into cement-based material to enhance the bonding strength. Their study provided insights into the bond strengthening mechanism in water-based drilling fluid, and can help cementing specialists to customise preflushes to enhance the cementation strength of the second cementing interface, thereby achieving better annular sealing and ensuring long-term effective isolation. In terms of injection technology, Yang Mou et al. [22] adopted computational fluid dynamics (CFD) and optimised the injection sequence of the pad fluid to improve the displacement efficiency. The results showed that the injection sequence of

the flushing fluid–spacer led to the displacement efficiency being as high as 89.67%. By increasing the dosage of cement slurry to one and a half annular volume, the displacement efficiency reached 95.16%. Li, Jin et al. [23] proposed a new evaluation system for the hydraulic sealing capability (HSC) of the cementing interface. The study results showed that the injection sequence of the pad fluid, flushing fluid–spacer–flushing fluid, could improve the HSC of the cement-formation interface. Additionally, 15–20 min was deemed to be the best flushing time. In summary, many studies have focused on the design of the pad fluid, and thoroughly described the system performance [24]. However, in terms of technology design, they mainly focus on the influence of the pad fluid on the displacement efficiency. When studying the injection sequence, the dosage of pad fluid was equal to the annular volume, which had a certain discrepancy from the dosage of pad fluid used in the actual project. The dosage of the pad fluid was determined by the optimal flushing fluid time, which lacked a consideration of operation safety. Therefore, we believe that the dosage of the pad fluid and the injection sequence should be comprehensively studied from the perspective of safety and the quality of cementing operations.

Addressing the shortcomings of previous studies, a displace motion model was established based on computational fluid dynamics (CFD) theory and the VOF, volume of fluid method, while a more refined annular equivalent circulating density (ECD) calculation model was established based on high-temperature and high-pressure rheological experimental results. Numerical simulations were conducted to study the effect of the dosage and injection sequence of the pad fluid on the displacement efficiency and ECD, and the findings were applied to the wells in the field. The study results can help guide the scientific and rational design of pad fluid in engineering, and lay a theoretical foundation for ensuring the safety and quality of cementing operations.

2. Analysis of Rheological Properties of Annulus Fluid

Examining the rheological properties of the annulus fluid is the prerequisite for studying the downhole flow of the cementing fluid. In this study, the drilling fluid and cement slurry of well X in an eastern oilfield were used to conduct rheological experiments under high temperature and high pressure to study the rheological properties of the cementing fluid under different temperature and pressure conditions. The objective was to better restore the actual fluid state of the horizontal section.

Figures 2 and 3, respectively, show the relationship between the rate of shear and shear stress measured in rheological experiments under high temperature and high pressure for drilling fluid and cement slurry. It is evident that the temperature has a stronger impact on the shear viscosity of both the drilling fluid and cement slurry, while pressure has less impact. Three common rheological models (Bingham model, power-law model, and Herschel-Buckley model described by Equations 1, 2, and 3, respectively) were used to fit the experimental data, and the most suitable rheological model was selected according to the correlation coefficient R^2 of the fitting results. The behaviour of the drilling fluid was best fitted with the Bingham model, and the cement slurry was best fitted with the Herschel-Buckley model. According to the temperature and pressure at the downhole of well X, the rheological parameters (see Table 1 below) fitted at 90 °C, –70 MPa were selected as the basis for the calculation of the follow-up displacement model and ECD.

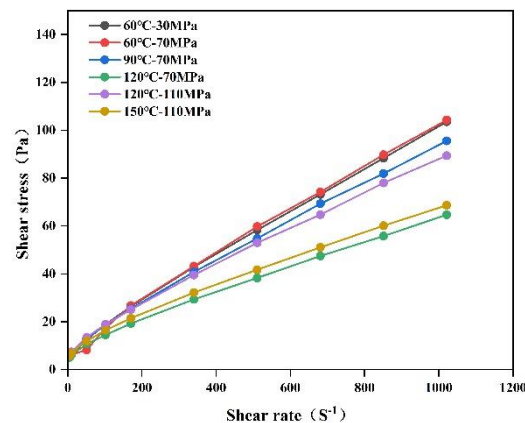


Figure 2. Rheological properties of drilling fluid.

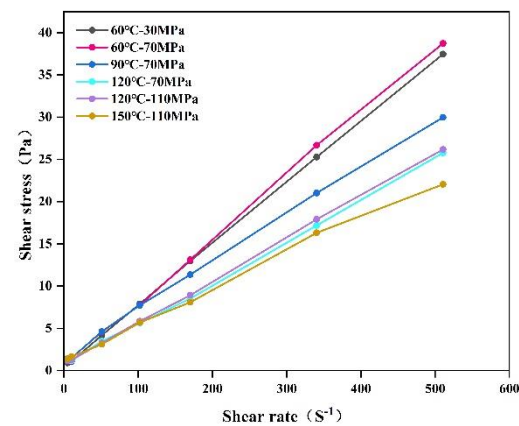


Figure 3. Rheological properties of cement slurry.

Table 1. Rheological models and rheological parameters.

| | Rheological Model | Fluidity Index | Yield Stress (Pa) | Consistency Index (Pa s ⁿ) | Density (g/cm ³) |
|----------------|-------------------|----------------|-------------------|--|------------------------------|
| Drilling fluid | Bingham | / | 7.59 | 0.057 | 1.75 |
| Spacer | Bingham | / | 0.39 | 0.21 | 1.8 |
| Flushing fluid | Herschel-Buckley | 0.823 | 0 | 0.43 | 1.05 |
| Cement Slurry | Herschel-Buckley | 0.74 | 1.09 | 0.08 | 1.9 |

(1) Bingham model

The mathematical expression of the Bingham equation is:

$$\tau = \tau_0 + \eta_p \dot{\gamma} \quad (1)$$

where τ is the shear stress, Pa; $\dot{\gamma}$ is the shear rate, s⁻¹; τ_0 is the yield point, Pa; and η_p is the plastic viscosity, Pa·s.

The Bingham equation is also called the plastic equation. Its functional relationship is a straight line with yield points, which is used to describe the rheological rules of the plastic fluid. A Bingham fluid can be considered as an idealised fluid, which can only flow under the action of a certain external force. Therefore, it cannot reflect the rheological rules of the fluid under low shear rate.

The yield point τ_0 and plastic viscosity η_p of the plastic fluid are constants, which do not vary with the shear rate and shear stress, i.e., for a given plastic fluid, τ_0 and η_p are

constants. Thus, the yield point τ_0 and plastic viscosity η_p are two important parameters that reflect the rheological properties of plastic fluids.

(2) Power-law model

The mathematical expression of the power-law equation is:

$$\tau = K\dot{\gamma}^n \quad (2)$$

where K is the consistency index, $\text{Pa}\cdot\text{s}^n$; and n is the fluidity index, which is dimensionless.

The power-law equation, also known as the pseudoplastic equation, is used to describe the flow characteristics of a pseudoplastic fluid and dilatant fluid. In the equation, K is the consistency index, which reflects the internal friction for laminar flow among solid microparticles, liquid phases, and between microparticles and liquid phases. Additionally, n is the fluidity index of the fluid, which reflects the non-Newtonian nature of the fluid. When $n = 1$, the fluid is a Newtonian fluid. For a smaller value of n , the non-Newtonian characteristics and shear thinning properties are stronger, and the velocity profile of the fluid is gentle. The power-law equation cannot reflect the gel strength of fluids and is also inapplicable of determining low shear rates.

(3) Herschel-Buckley equation

The mathematical expression of the Herschel-Buckley equation is:

$$\tau = \tau_y + K'\dot{\gamma}^{n'} \quad (3)$$

where τ_y is the gel strength, Pa; K' is the consistency index, $\text{Pa}\cdot\text{s}^n$; and n' is the fluidity index, which is dimensionless.

The Herschel-Buckley equation (H-B) is also called the power-law equation with gel strength. The equation is a three-parameter model. Although the values of K' and n' are different from those of fluids obeying the power law, they have the same meaning. As Equation (3) is a transcendental equation with three undetermined coefficients, according to the function approximation principle, for more undetermined coefficients in the approximation function, the degree of approximation is higher. As the Herschel-Buckley equation has better adaptability for low, medium, and high shear rates, it has greater advantages over the Bingham equation and the power-law equation.

3. Calculation Model

Under the influence of gravity and the casing running process, the casing of horizontal wells has serious eccentricity issues. In this study, we established a physical model based on a wellbore in a horizontal section. The model is shown in Figure 4. The relevant parameters are as follows: length of the horizontal section is 30 m, dimension of the borehole is 215.9 mm, casing dimension is 139.7 mm, and the eccentricity is 0.6. ANSYS/FLUENT software was used to solve the flow field.

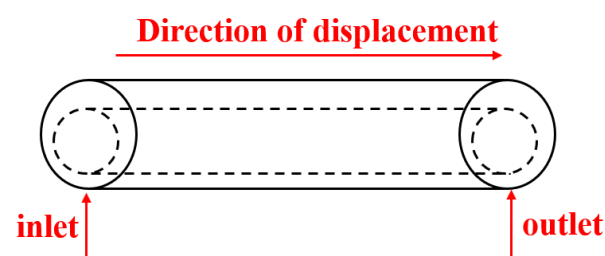


Figure 4. Spatial geometry model.

Initially, the drilling fluid filled the entire annulus. The pad fluid and cement slurry were injected sequentially from the inlet to displace the drilling fluid. The inlet of the calculation model was set as the boundary condition of the velocity inlet, and the outlet end

was set as the boundary condition of free flow. The roughness of both the casing wall and shaft wall of the wellbore were not considered, and the no-slip wall boundary condition was adopted.

In addition, the creation of the computational model and the meshing is very important for the accuracy of the computation [25–27], and we have adopted a local grid encryption to mesh the created model as shown in Figure 5 below.

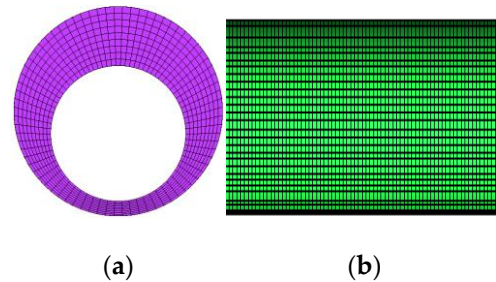


Figure 5. Grid model. (a) Eccentric annular side view, (b) eccentric annular front view.

3.1. Displacement Motion Model

According to the fluid flow characteristics in the cementing annulus (incompressible viscous fluid), the N-S equation is used as the governing equation:

$$\frac{\partial v}{\partial t} + (v \cdot \nabla)v = f + \frac{1}{\rho} \nabla \cdot \sigma \quad (4)$$

where v is the velocity, m/s; f is the body force per unit mass of fluid, m/s^2 ; ρ is the fluid density, kg/m^3 ; σ is the total stress, Pa; and t is time, s.

Momentum equation

$$\frac{\partial(\rho v)}{\partial t} + \text{div}(\rho v v) = \rho g + \text{div} T \quad (5)$$

where ρ is the fluid density, kg/m^3 ; t is the time, s; v is the velocity vector; g is the acceleration of gravity; $\text{div} T$ is the surface tension term; and T is the stress tensor matrix, including normal stress and tangential force.

The phase interface tracking of each calculation unit is achieved by volume of fluid (VOF). VOF defines the volume fraction of a certain fluid in any calculation unit. In order to satisfy the law of conservation of mass, a_i should satisfy:

$$\frac{\partial a_i}{\partial t} + v \nabla a_i = 0 \quad (6)$$

$$a_1 + a_2 + a_3 + a_4 = 1 \quad (7)$$

where a_i ($i = 1, 2, 3, 4$) is the volume fraction of each phase, $a_i = 0$ denotes that there is no phase i in the governing volume, and $a_i = 1$ denotes that only phase i is contained in the governing volume.

The mixing of multiphase flow in the annulus can be described by the convection–diffusion equation:

$$\frac{\partial c_k}{\partial t} + u_i \frac{\partial c_k}{\partial x} + u_j \frac{\partial c_k}{\partial y} = \nabla \cdot [D_k(c, u) \nabla c_k] + r_k \quad (8)$$

where $D_k(c, u)$ is the molecular diffusion coefficient of component k ; r_k is the quantity of component k generated via chemical reaction per unit time per unit volume space, mol; and c_k is the mass concentration of component k , mol/L.

3.2. Annulus ECD Calculation Model

The dynamic equivalent circulating density (ECD) is an important parameter to control the fluid column pressure of the annulus. It is mainly composed of hydrostatic fluid column pressure and annular circulation pressure loss. On site, the expression of ECD is:

$$ECD = \frac{P_{hy} + P_{wh} + P_{-f}}{gH} \quad (9)$$

In the equation, ECD is the equivalent circulating density, g/cm^3 ; P_{hy} is the hydrostatic column pressure, Pa; P_{-f} is the annular pressure loss at depth H of the well, Pa; P_{wh} is the back pressure at the wellhead, Pa; and H is the well depth, m.

Meanwhile, it is necessary to establish a calculation model for the pressure loss of annular flow, which is expressed as:

$$P_{-f} = \frac{0.2f\rho v^2}{Dh - Dp}H \quad (10)$$

where f is the hydraulic friction factor of the pipeline, dimensionless; ρ is the fluid density, g/cm^3 ; v is the average flow velocity, m/s; Dh is the inner diameter of the borehole, cm; and Dp is the inner diameter of the casing, cm.

4. Results and Analysis

Displacement efficiency is the basic premise for ensuring cementing quality, while ECD is the foundation for ensuring cementing safety. During the displacement operation, the annulus ECD should be strictly controlled within the safety density window. If it is greater than the equivalent density of formation fracture (the upper limit of the window), lost circulation can occur. However, if it is less than the equivalent density of collapse pressure of the formation (the lower limit of the window), hole collapse can occur. In this section, we created a full three-dimensional cementing displacement model for horizontal wells to display the displacement process in real time. Using a single factor to control variables, we focused on studying the effects of pad fluid amount and injection sequence on displacement efficiency and ECD.

4.1. The Effects of Dosage and Injection Sequence of Pad Fluid on the Displacement Efficiency and ECD

When studying the injection sequence of the pad fluid, the dosage of the spacer was 0.5 times of the annular volume of the cementing segment, and the dosage of the flushing fluid was 0.1 times the annular volume of the cementing segment. Figure 6 shows the volume fractions of each phase fluid at the final moment with different annular volume multiples occupied by different dosages of spacers. Figure 7 shows the volume fractions of each phase fluid at the final moment with different annular volume multiples occupied by different dosages of flushing fluid. Figure 8 shows the colour maps of the volume fractions of the wide side and narrow side of the annulus at the end of displacement with 0.6 times the dosage of pad fluid. Figure 8 shows the colour map of the axial velocity distribution of the wide side and narrow side of the annulus at the end of displacement with 0.6 times the dosage of pad fluid.

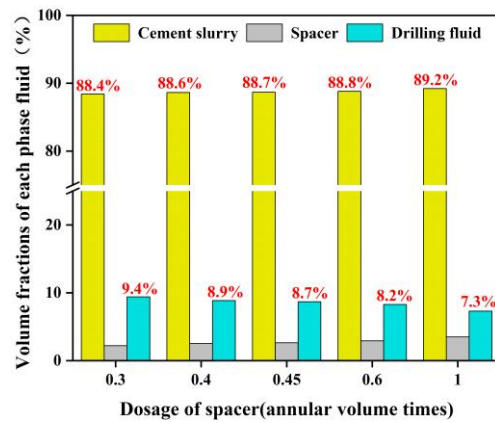


Figure 6. Volume fractions of each phase fluid in annular at the end of displacement with different dosages of spacer. (Volume fractions of cement slurry means displacement efficiency, same on the right side).

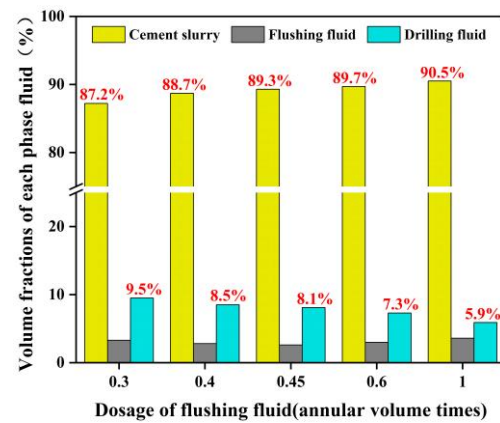


Figure 7. Volume fractions of each phase fluid in annular at the end of displacement with different dosages of flushing fluid.

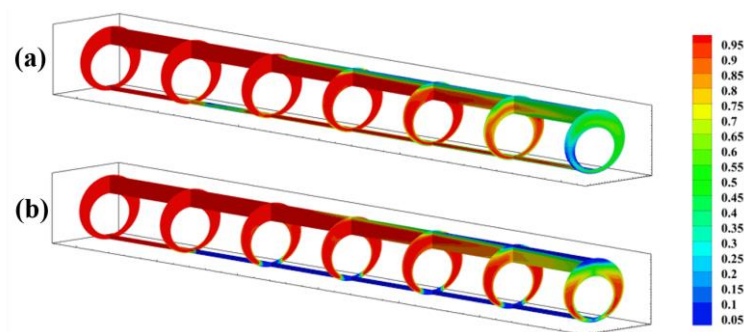


Figure 8. Colour map of cement slurry volume distribution at the end of displacement. ((a,b) refer to the injection of 0.6 times of the annular volume of flushing fluid and spacer).

As seen in Figures 6 and 7, as the dosage of the pad fluid increases, the displacement efficiency increases gradually along with a gradual decrease in the retention of the drilling fluid. When using a spacer in the pad fluid, as the dosage is increased from 0.3 times the annular volume of the cementing segment to 1.0 times, the displacement efficiency can be increased by 0.8%, while the retention of the drilling fluid can be reduced by 2.1%. When using flushing fluid in the pad fluid, as the dosage is increased from 0.3 times the annular volume of the cementing segment to 1.0 times, the displacement efficiency can be increased by 3.2%, while the retention of the drilling fluid can be reduced by 3.6%. Comparing the

different annular volume multiples of the pad fluid and flushing fluid, it is evident that when the dosage of pad fluid injection is less than 0.4 times the annular volume of the cementing segment, the displacement performance after adding a spacer in the pad fluid is better than that of the flushing fluid. When the dosage of pad fluid injection is greater than 0.4 times the annular volume of the cementing segment, the displacement performance after adding flushing fluid in the pad fluid is better than that of the spacer. The reason is that when the injection dosage of the flushing fluid is less than a certain multiple, the density contrast plays a major role in the displacement performance. When the dosage of the flushing fluid reaches a certain multiple, the injection of the flushing fluid flushes and dilutes the drilling fluid. At this time, the cement slurry can displace the drilling fluid more effectively.

Figures 8 and 9 show the section of the wellbore along the middle position in the upward axial direction. As can be seen from the colour map of the volume distribution of the cement slurry at the end of displacement (Figure 8), when pad fluid equal to 0.6 times the annulus is injected, the injection of the flushing fluid can better displace the remaining drilling fluid in the narrow gap of the annulus, and more effectively fill cement slurry at the narrow edge compared to the spacer. Comparing with the colour map of the axial velocity distribution at the end of the displacement (Figure 9), it is observed that the flow velocity in the wide side of the annulus is considerably higher than that in the narrow side. When injecting the flushing fluid, the flow velocity at the end of the narrow side of the annulus is significantly improved, with the flow velocity at the initial end of the narrow side being almost the same.

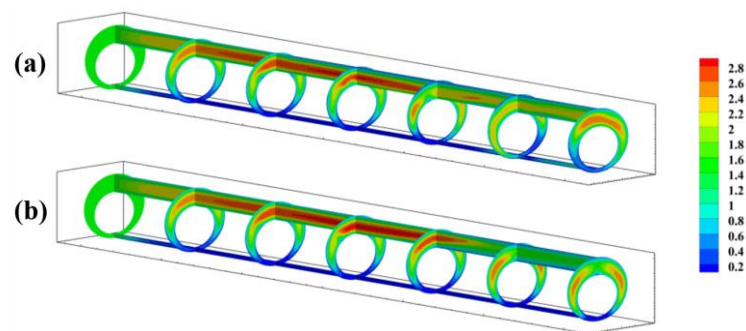


Figure 9. Colour map of axial velocity distribution at the end of displacement. ((a,b) refer to the injection of 0.6 times of the annular volume of flushing fluid and spacer).

By calculating the ECD of different pad fluid dosages (as shown in Figures 10 and 11 above), with an increase in the dosage of the spacer, the ECD of the entire well gradually increases, and with the increase in the dosage of flushing fluid, the ECD gradually decreases. As the well in the current study uses high-density drilling fluid, the dosage of the spacer has an insignificant effect on ECD. With the change in the dosage of spacer from 0.3 times the annular volume to 1.0 times, the difference of the annular volume ECD at the downhole is 0.017 g/cm^3 . However, with the change in the dosage of the flushing fluid from 0.3 times the annular volume to 1.0 times, the difference in the annular volume ECD at the downhole is 0.28 g/cm^3 . Therefore, it is necessary to select the most appropriate dosage multiple of the pad fluid between the fracture pressure coefficient and leakage pressure coefficient to ensure no leakage or collapse, and also to maximise the displacement efficiency.

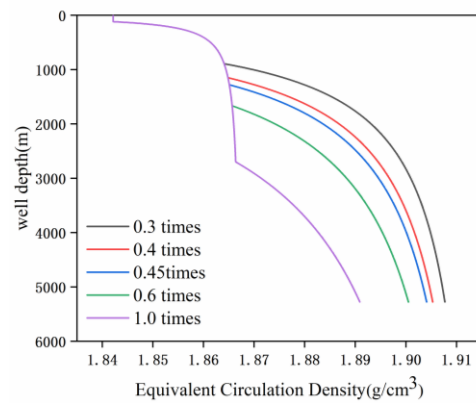


Figure 10. ECD with different dosages of spacer. (1.0 times means sealing section annular volume, same on the right).

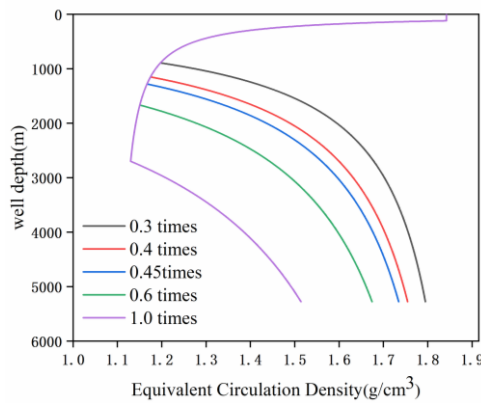


Figure 11. ECD with different dosages of flushing fluid.

4.2. The Effects of Injection Sequence of Pad Fluid on Displacement Efficiency and ECD

When studying the injection sequence of the pad fluid, the overall dosage of the spacer was 0.5 times the annular volume of the cementing segment, and the overall dosage of the flushing fluid was 0.1 times the annular volume of the cementing segment. Figure 10 shows the fluid volume fraction of the four-phase fluid, at the final moment, with different injection sequences of the pad fluid, and Figure 12 shows the ECD with different injection sequences of the pad fluid.

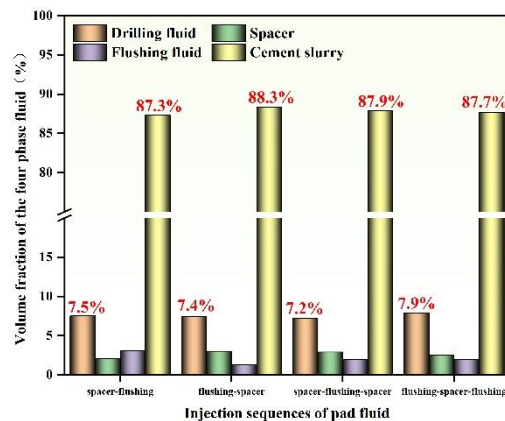


Figure 12. Volume fractions of four-phase fluid with different injection sequences of pad fluid.

From Figure 12, it is evident that when the injection sequence of the pad fluid is flushing fluid–spacer, the highest displacement efficiency is 88.3%, while when the injection

sequence is spacer–flushing fluid, the lowest efficiency is 87.3%, which is 1% lower than that in the former sequence. The reason is that when the injection sequence of the pad fluid is flushing fluid–spacer, the injection of the flushing fluid can flush and dilute the drilling fluid, and also dilute a part of the later injected high-density spacer. Hence, the pad fluid can be displaced effectively when cement slurry is injected, thereby achieving the highest displacement efficiency. When the injection sequence of the pad fluid is spacer–flushing fluid, although the high-density spacer can generate a density contrast to effectively displace the drilling fluid, the subsequently injected low-density flushing fluid dilutes not only the spacer, but also the subsequently injected cement slurry, leading to reduced displacement efficiency of the cement slurry.

From Figure 13, it can be concluded that under the condition of injecting the same dosage of pad fluid, irrespective of the sequence used, the final downhole pressure remains constant. The ECD at the top of the hole increases or decreases with different injection sequences. In the column structure of spacer–flushing fluid–cement slurry, the annulus equivalent density varies from 1.949 g/cm³ to 1.993 g/cm³. The window is 0.044 g/cm³. However, in the column structure of flushing fluid–spacer–cement slurry, the annulus equivalent density varies from 1.881 g/cm³ to 1.967 g/cm³. The window is 0.086 g/cm³. Comparing the changes in annulus equivalent density of these two column structures, the sequence of spacer–flushing fluid has a smaller range of impact on the annulus ECD. Therefore, using this structure, the formation pressure can be adjusted and balanced more effectively.

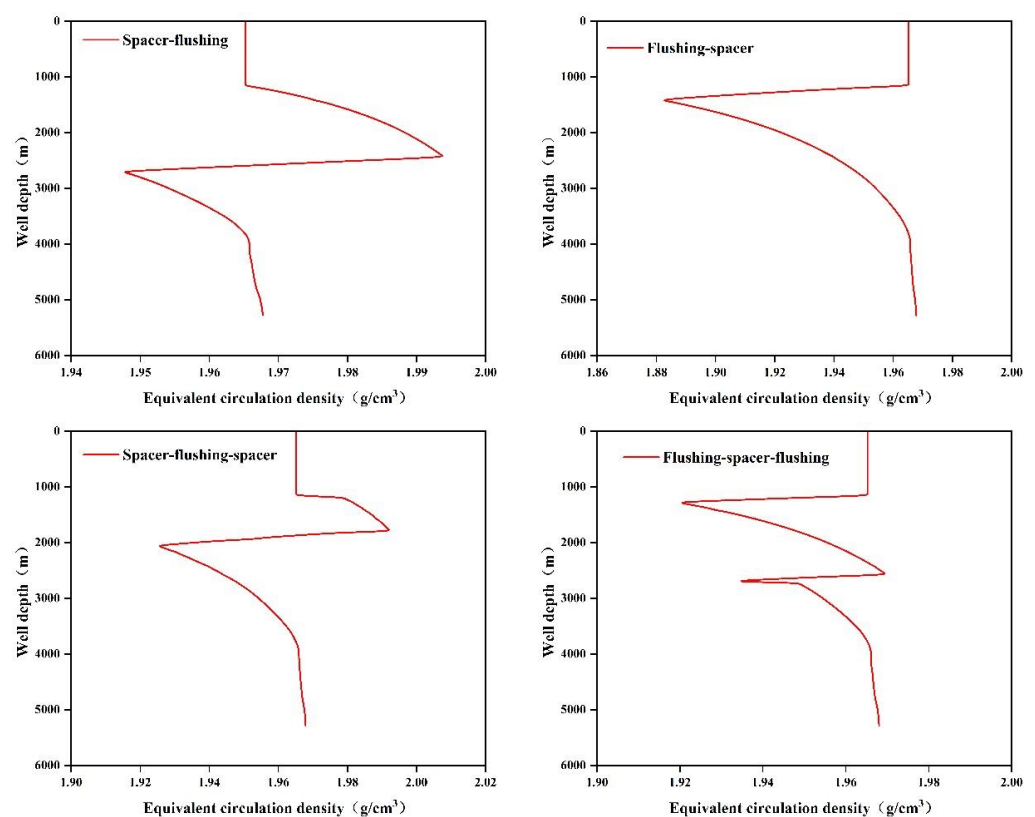


Figure 13. ECD with different injection sequences of pad fluid.

5. Application on Site

In order to further verify the accuracy of understanding of pad fluid design, we considered the casing cement of a horizontal shale oil well in eastern China as an example. This well uses sylvite-system drilling fluid, which has a density of 1.55 g/cm³. The borehole size in the reservoir is 215.9 mm and the casing size is 139.7 mm. The drilling depth is 3035.4–6104 m. The main cementing difficulties of this well are as follows: (1) the length

of the horizontal segment is 1871 m, and the angle of inclination exceeds 90° at the depth from 5188 m to 6108 m, with a maximum of 97° . Meanwhile, the borehole trajectory has an upward trend, and there can be keyways, which affect the cementing displacement efficiency; (2) the drilling fluid has a high yield point and high viscosity, and is difficult to wash off, which affects the cementing displacement efficiency and interface cementation quality; (3) the cementing safety density window is narrow, and the one-time cementing segment is long. There is a risk of leakage.

In order to improve the cementing quality of this well and guarantee the operation safety and displacement efficiency, the original design scheme of the cementing operation of this well was optimised in the current study. The schemes before and after optimisation are, respectively, Scheme 1 and 2, as shown in Table 2. After optimisation, the dosage of pad fluid was increased, and the injection sequence was changed. The theoretically calculated displacement efficiency was increased by 2%, which was consistent with the aforementioned conclusions. Further calculation of the annulus ECD at the end of the displacement is shown in Figure 14. The ECDs are all within the safety density window, which can guarantee operation safety.

Table 2. Design scheme of pad fluid.

| Scheme | Dosage of Spacer (m^3) | Dosage of Flushing Fluid (m^3) | Injection Sequence | Displacement Efficiency |
|----------|-----------------------------------|---|-----------------------|-------------------------|
| Scheme 1 | 30 | 8.7 | Spacer–flushing fluid | 89.6% |
| Scheme 2 | 35 | 10.7 | Flushing fluid–spacer | 91.6% |

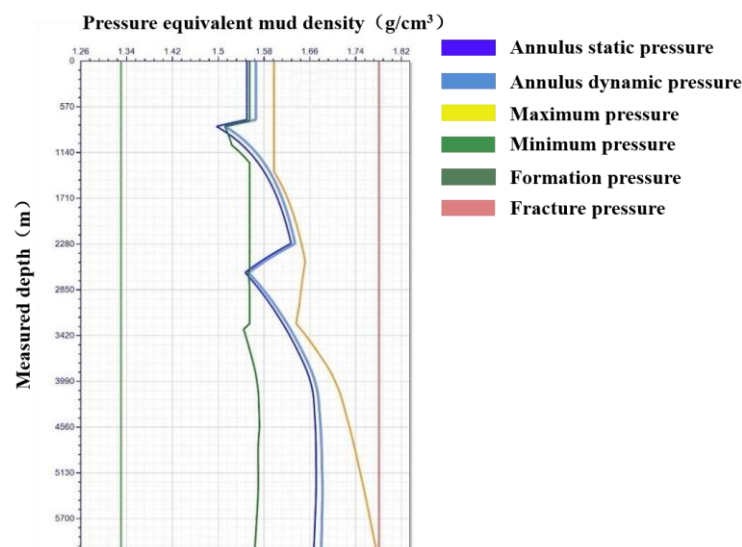


Figure 14. Distribution diagram of annulus ECD at the end of displacement.

The process of the cementing operation of the reservoir casing section in this well is shown in Figure 15. The construction was carried out during 03:15–06:42. Section A,B was the flushing pipeline and was at the pressure test stage. The pressure increased up to 54 MPa, and was stabilised for 5 min. Subsequently, 8.7 m^3 of flushing fluid, 35 m^3 of spacer, 2.0 m^3 of flushing fluid, and 68.3 m^3 of cement slurry were sequentially injected in section B,C. Clean water was injected after the point C. Then, the displacement process started. The flow rate was reduced in section D,E to prepare for bumping in Section F,G. Section H,I included emptying and waiting for cement setting with annular pressure at 4 MPa. The entire operation process was safe, and cementing was successfully completed. After 48 h of waiting for the cement to set, the results of sonic amplitude logging showed

that the pass rate of the first interface was 100%, and the pass rate of the secondary interface was 70.6%, which was 8.8% higher than the pass rate of the secondary interface of the adjacent well. The cementing quality was improved significantly.

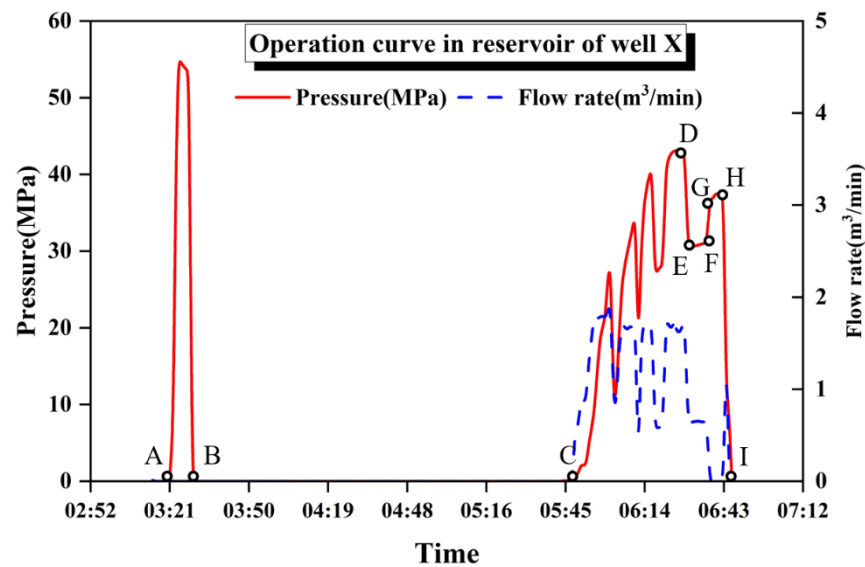


Figure 15. Cementing operation curve of the reservoir casing section. (The letters A-I are used to better describe the process).

6. Conclusions

In this study, we analysed the rheological properties of the annulus fluid. The Herschel-Buckley model was adopted as the rheological equation. Through the development of a displacement motion model and annulus ECD calculation model and by adopting numerical simulations, the effect of the dosage and injection sequence of the pad fluid on the displacement efficiency and annulus ECD were studied. The main conclusions are as follows:

- (1) As the dosage of pad fluid increases, the retention of drilling fluid in the annulus decreases and the displacement efficiency increases. When the pad fluid is composed completely of flushing fluid, the displacement efficiency is better than when it is composed completely of spacer. By increasing the dosage of flushing fluid from 0.3 times the annular volume to 1.0 times, the displacement efficiency can be increased by 3.3%, and the retention of the drilling fluid is reduced by 3.6%. However, the annulus dynamic pressure is considerably reduced, which increases the risk of leakage during cementing operation. Therefore, it is necessary to ensure that the annulus dynamic pressure is within the range of the safety density window while increasing the dosage of flushing fluid during operations.
- (2) The injection sequence of the pad fluid has different effects on the displacement efficiency. The minimum displacement efficiency of 87.3% is achieved by the injection sequence of spacer–flushing fluid, and the maximum displacement efficiency of 88.3% is achieved by the injection sequence of flushing fluid–spacer. When improving the displacement efficiency by increasing the dosage of flushing fluid, a section of high-density spacer can be added subsequently to increase the annulus ECD. This not only ensures the best displacement effect, but also reduces operation risks.
- (3) Applications on site show that increasing the dosage of pad fluid and using the injection sequence of spacer–flushing fluid can improve the displacement efficiency, while guaranteeing the safety of cementing operations. This study mainly focuses on the application of technology research on horizontal wells. The obtained results have important theoretical significance and application value that can provide guidance for the design optimisation of operations on site.

Based on the research results, we provide a risk rating table, as shown in Table 3 below.

Table 3. Risk rating table.

| Number | Pre-Fluid Structure | | Replacement Quality | Risk Level | Control Measures |
|--------|-------------------------------|-----------------------|---------------------|------------|---|
| | Dosage (Annular Volume Times) | Injection Sequence | | | |
| 1 | >1.0 | Flushing fluid | High | High | Combined with fine pressure control cementing technology at the wellhead Increase the dosage |
| 2 | 0.4–1.0 | | High | Mid | |
| 3 | <0.4 | | Low | Low | |
| 4 | >1.0 | Spacer | High | Mid | / |
| 5 | <=1.0 | | Mid | Low | |
| 6 | 0.6 | Flushing fluid–spacer | Mid | Low | Increase the dosage |
| 7 | | Spacer–flushing fluid | Low | Low | Change the injection sequence or increase the dosage |

Author Contributions: Conceptualization, B.Q. and Z.L.; Methodology, J.S.; Funding acquisition, B.Q.; Supervision, J.F.; Validation, J.F.; Visualization, J.S.; Project administration, Z.L.; Resources, Z.L.; Writing—original draft, X.Y. and X.W.; Formal analysis, X.Y.; Data curation, F.Y.; Writing—review & editing, X.W.; All authors have read and agreed to the published version of the manuscript.

Funding: This research work was supported by the scientific research starting project of SWPU (No. 2021QHZ029), the science and technology project of the CNPC Bohai Drilling Engineering Company Limited (No. 2021ZD24Y-02), the study on structure design and flow model of stepless variable density cement slurry column (BHZT-CJ2-2022-JS-215), and the National Natural Science Foundation of China (52274010).

Data Availability Statement: Not applicable.

Conflicts of Interest: The authors declare no conflict of interest.

References

- Hou, Z.; Luo, J.; Xie, Y.; Wu, L.; Huang, L.; Xiong, Y. Carbon Circular Utilization and Partially Geological Sequestration: Potentialities, Challenges, and Trends. *Energies* **2023**, *16*, 324. [CrossRef]
- Xie, Y.; Qi, J.; Zhang, R.; Jiao, X.; Shirkey, G.; Ren, S. Toward a Carbon-Neutral State: A Carbon-Energy-Water Nexus Perspective of China's Coal Power Industry. *Energies* **2022**, *15*, 4466. [CrossRef]
- Wikipedia. Deepwater Horizon Oil Spill. 2023. Available online: https://en.wikipedia.org/wiki/Deepwater_Horizon_oil_spill (accessed on 9 March 2023).
- Wikipedia. Aliso Canyon Gas Leak. 2022. Available online: https://en.wikipedia.org/wiki/Aliso_Canyon_gas_leak (accessed on 9 March 2023).
- Wu, X.; Liu, J.; Li, Z.; Song, W.; Liu, Y.; Shi, Q.; Chen, R. Failure Analysis of Cement Sheath Mechanical Integrity Based on the Statistical Damage Variable. *ACS Omega* **2023**, *8*, 2128–2142. [CrossRef] [PubMed]
- Tan, C.; Wang, M.; Chen, R.; You, F. Study on the Oil Well Cement-Based Composites to Prevent Corrosion by Carbon Dioxide and Hydrogen Sulfide at High Temperature. *Coatings* **2023**, *13*, 729. [CrossRef]
- Dou, N.; Wang, Z.; Leng, G.; Liu, H.; Hu, Z.; Jiang, K. Development and Performance Evaluation of Novel Solid-Free Epoxy Resin System for Remediation of Sustained Casing Pressure. *Energies* **2023**, *16*, 2771. [CrossRef]
- Zhao, L.; Li, N.; Yang, J.; Wang, H.; Zheng, L.; Wang, C. Alkali-Resistant and pH-Sensitive Water Absorbent Self-Healing Materials Suitable for Oil Well Cement. *Energies* **2022**, *15*, 7630. [CrossRef]
- Liu, H.; Qin, J.; Zhou, B.; Liu, Z.; Yuan, Z.; Zhang, Z.; Ai, Z.; Pang, X.; Liu, X. Effects of Curing Pressure on the Long-Term Strength Retrogression of Oil Well Cement Cured under 200 °C. *Energies* **2022**, *15*, 6071. [CrossRef]
- Lobastov, D.; Nafikova, S.; Akhmetzianov, I.; Zaripov, S.; Krivolapov, D. Collaborative Approach Overcomes Cementing Challenges in Narrow Pressure Window Environment. In Proceedings of the SPE Russian Petroleum Technology Conference, Virtual, 12–15 October 2021; IADC/SPE: Moscow, Russia, 2021.
- Isgenderov, I.; Bogaerts, M.; Osayande, V. ECD Management Solves Lost Circulation Issues in Cementing Narrow Pressure Window: A Case Study. In Proceedings of the IADC/SPE Asia Pacific Drilling Technology Conference, Bangkok, Thailand, 25–27 August 2014.
- Marriott, J.T.; Griffith, G.; Mallett, H.C. Foamed Conventional Lightweight Cement Slurry for Ultralow Density and Low ECDs Solves Lost-Circulation Problem across Coal Formations: A Case History. In Proceedings of the SPE Annual Technical Conference and Exhibition, Dallas, TX, USA, 9–12 October 2005.
- Zhang, H.; Guo, J.; Yang, L.; Wu, P.; Xue, H.; Yang, M. Optimization of cementing displacement efficiency based on circulation pressure of a shale gas horizontal well in low pressure and leakage formations. *Energy Rep.* **2022**, *8*, 11695–11706. [CrossRef]

14. Chengwen Wang, R.M.; Zehua, C.S.Y. Study on the Key Issue in the Application of Nanoemulsions in Preflush Spacer: Contamination of Cement Slurry by Nanoemulsions. *SPE J.* **2023**, *28*, 64–79. [[CrossRef](#)]
15. Bu, Y.; Li, Z.; Wan, C.; Li, H.A. Determination of optimal density difference for improving cement displacement efficiency in deviated wells. *J. Nat. Gas Sci. Eng.* **2016**, *31*, 119–128. [[CrossRef](#)]
16. Xue, L.; Han, H.; Zhang, M.; Fan, H. Cementing displacement efficiency analysis in long horizontal wells: An optimized numerical simulation approach. *J. Pet. Sci. Eng.* **2022**, *208*, 109393. [[CrossRef](#)]
17. Yu, H.; Dahi Taleghani, A.; Lian, Z. Impact of the dogleg geometry on displacement efficiency during cementing; an integrated modelling approach. *J. Pet. Sci. Eng.* **2019**, *173*, 588–600. [[CrossRef](#)]
18. Zhao, Y.; Wang, Z.; Zeng, Q.; Li, J.; Guo, X. Lattice Boltzmann simulation for steady displacement interface in cementing horizontal wells with eccentric annuli. *J. Pet. Sci. Eng.* **2016**, *145*, 213–221. [[CrossRef](#)]
19. Zulqarnain, M.; Tyagi, M. Development of simulations based correlations to predict the cement volume fraction in annular geometries after fluid displacements during primary cementing. *J. Pet. Sci. Eng.* **2016**, *145*, 1–10. [[CrossRef](#)]
20. Chen, E.; Wang, C.; Meng, R. A new type of cementation flushing fluid for efficiently removing wellbore filter cake. *Nat. Gas Ind. B* **2015**, *2*, 455–460. [[CrossRef](#)]
21. Lichinga, K.N.; Maagi, M.T.; Ntawanga, A.C.; Hao, H.; Gu, J. A novel preflush to improve shear bond strength at cement-formation interface and zonal isolation. *J. Pet. Sci. Eng.* **2020**, *195*, 107821. [[CrossRef](#)]
22. Yang, M.; Yang, L.; Li, Y.; Zhang, L.; Wang, C.; Zhou, L.; Yang, M. Improving displacement efficiency by optimizing pad fluid injection sequence during primary cementing of eccentric annulus in shale gas horizontal wells. *J. Pet. Sci. Eng.* **2021**, *204*, 108691. [[CrossRef](#)]
23. Li, J.; Liu, J.; Li, Z.; Liu, Y.; Wu, X.; Song, W. Influence Laws for Hydraulic Sealing Capacity in Shale Gas Well Cementing. *SPE Drill. Complet.* **2022**, *38*, 120–130. [[CrossRef](#)]
24. Curbelo, F.D.S.; Garnica, A.I.C.; Araújo, E.A.; Paiva, E.M.; Cabral, A.G.; Araújo, E.A.; Freitas, J.C.O. Vegetable oil-based preflush fluid in well cementing. *J. Pet. Sci. Eng.* **2018**, *170*, 392–399. [[CrossRef](#)]
25. Iraj, S.; Soltanmohammadi, R.; Munoz, E.R.; Basso, M.; Vidal, A.C. Core scale investigation of fluid flow in the heterogeneous porous media based on X-ray computed tomography images: Upscaling and history matching approaches. *Geoenergy Sci. Eng.* **2023**, *225*, 211716. [[CrossRef](#)]
26. Mahjour, S.K.; Santos, A.A.S.; da Graca Santos, S.M.; Schiozer, D.J. Selection of Representative Scenarios Using Multiple Simulation Outputs for Robust Well Placement Optimization in Greenfields. In Proceedings of the SPE Annual Technical Conference and Exhibition, Dubai, United Arab Emirates, 21–23 September 2021; Society of Petroleum Engineers: Richardson, TX, USA, 2021; p. SPE-206300-MS.
27. Soltanmohammadi, R.; Iraj, S.; De Almeida, T.R.; Munoz, E.R.; Fioravanti, A.R.; Vidal, A.C. *Insights into Multi-Phase Flow Pattern Characteristics and Petrophysical Properties in Heterogeneous Porous Media Second EAGE Conference on Pre-Salt Reservoir*; EAGE Publications BV: Utrecht, The Netherlands, 2021; pp. 1–5.

Disclaimer/Publisher's Note: The statements, opinions and data contained in all publications are solely those of the individual author(s) and contributor(s) and not of MDPI and/or the editor(s). MDPI and/or the editor(s) disclaim responsibility for any injury to people or property resulting from any ideas, methods, instructions or products referred to in the content.